

Electronic Supplementary Information

Synthesis, photophysical and non-linear optical properties of push-pull tetrazoles

Anna-Kay West, Lukas J. Kaylor, Mahamud Subir and Sundeep Rayat*

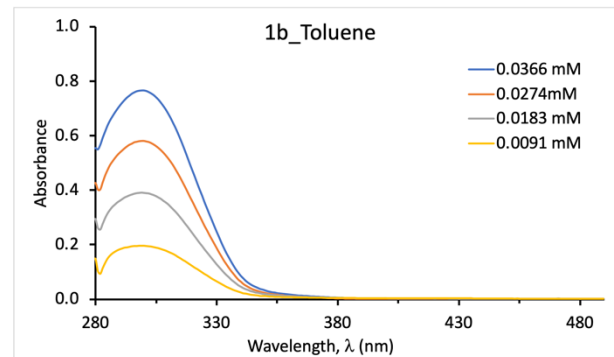
Department of Chemistry, Ball State University, Foundational Sciences Building, Muncie, IN 47306, United States.

Email: srayat@bsu.edu

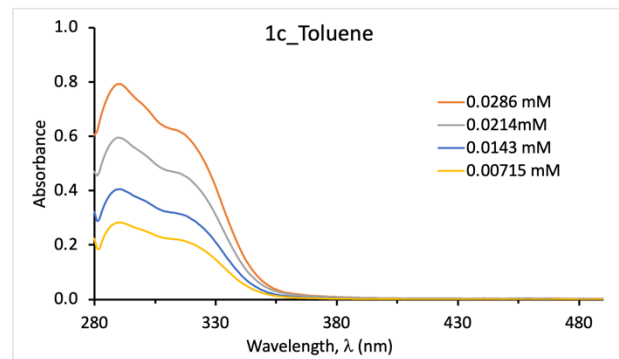
(a)

1a is insoluble in toluene

(b)



(c)



(d)

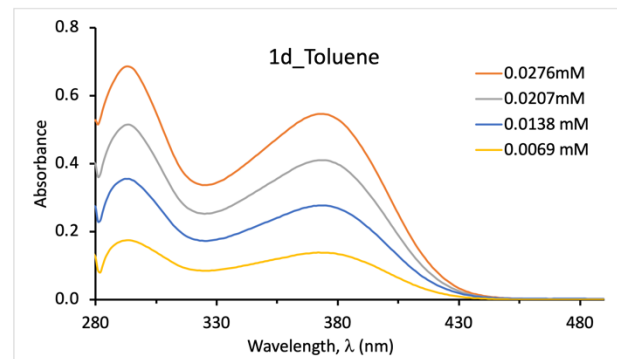


Figure S1. Absorption spectra of **1b – d** in toluene (x-axis begins at solvent cut-off).

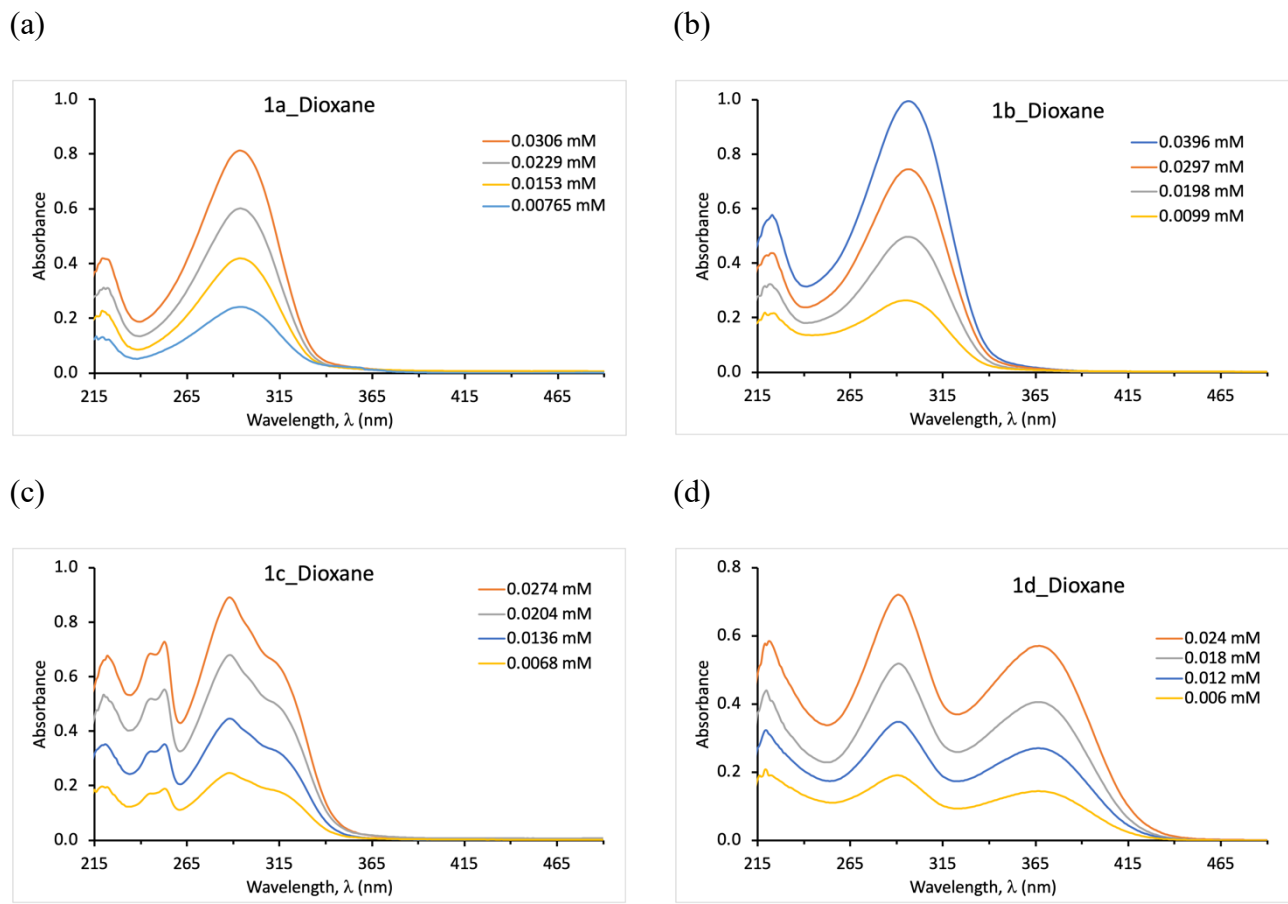


Figure S2. Absorption spectra of **1a – d** in 1,4-dioxane (x-axis begins at solvent cut-off).

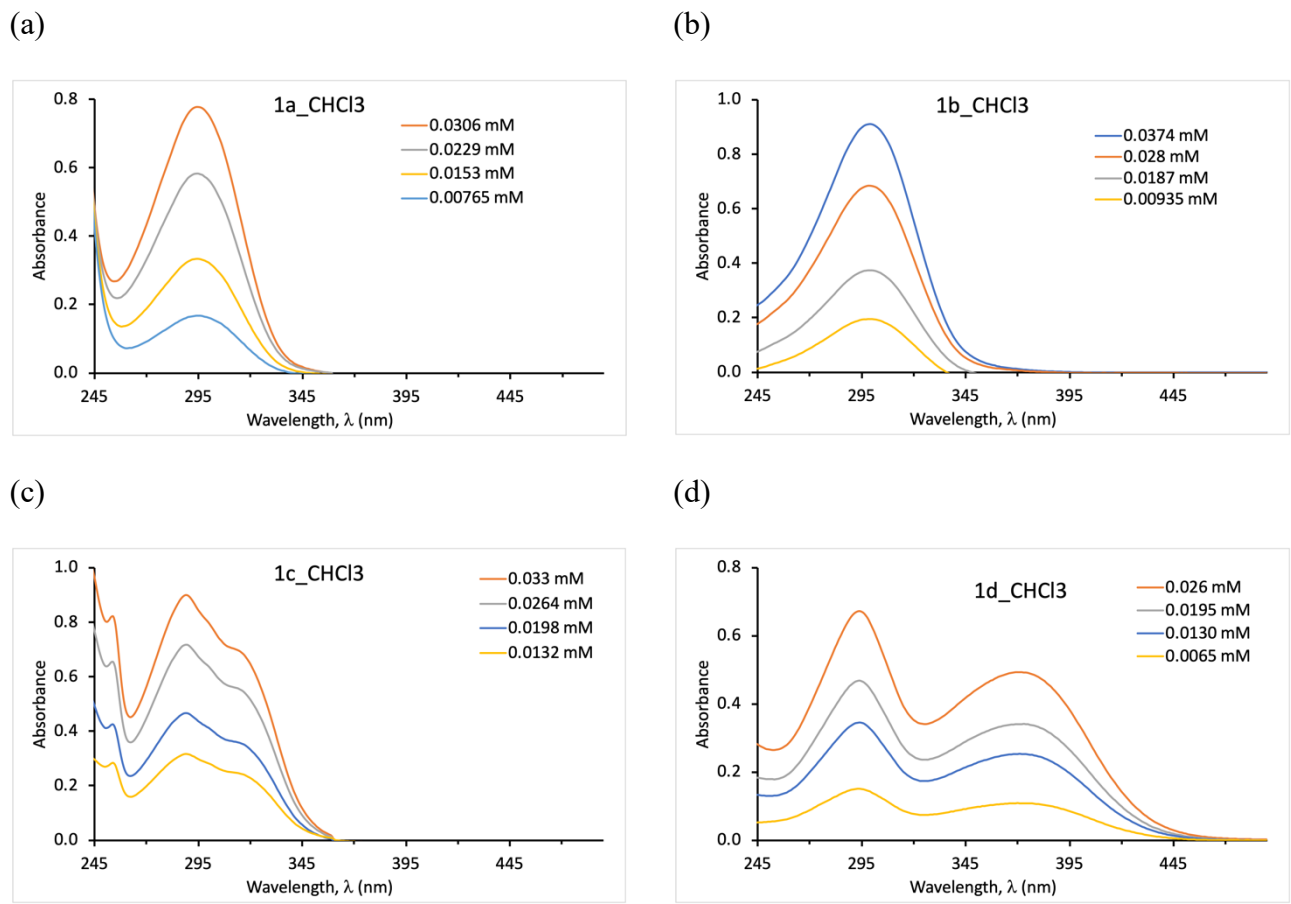


Figure S3. Absorption spectra of **1a – d** in chloroform (x-axis begins at solvent cut-off).

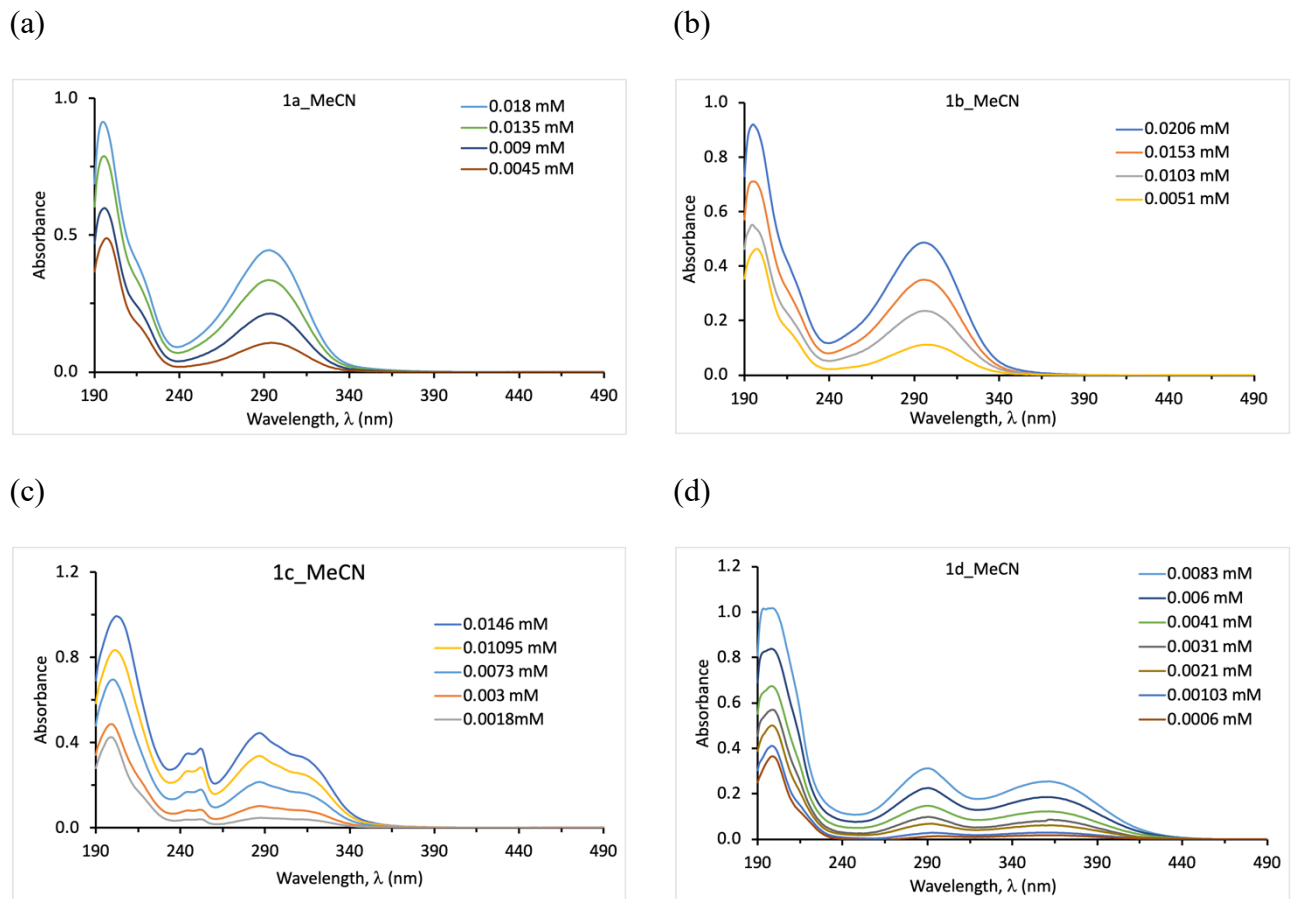


Figure S4. Absorption spectra of **1a – d** in acetonitrile.

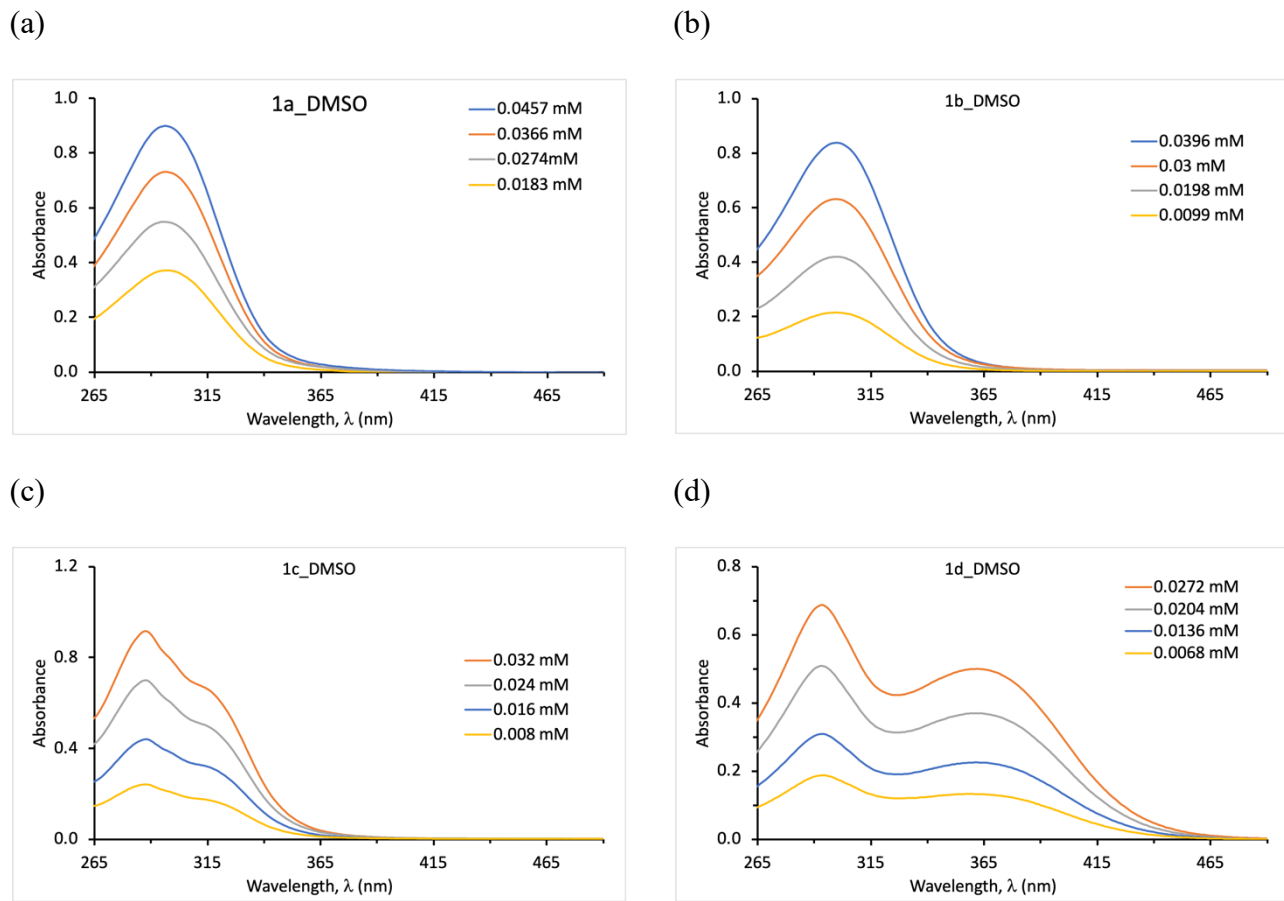


Figure S5. Absorption spectra of **1a – d** in DMSO (x-axis begins at solvent cut-off).

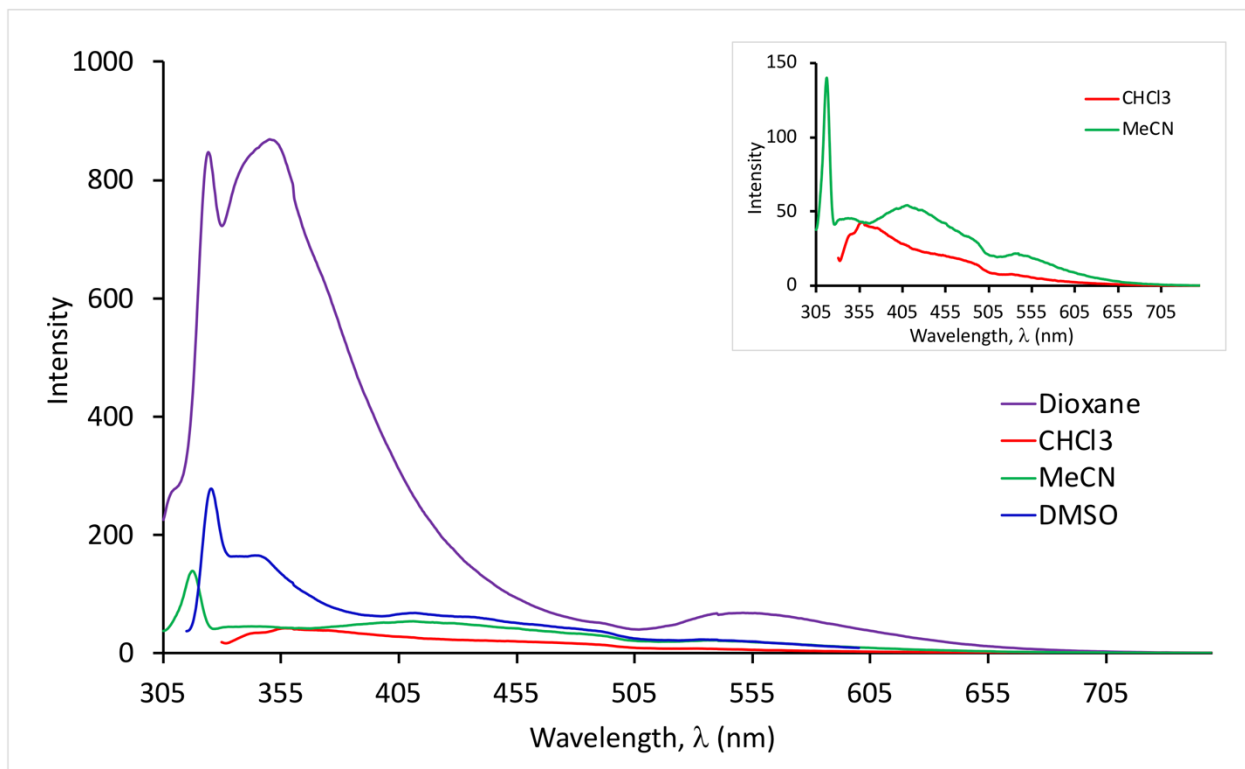


Figure S6. Emission spectra of **1a** in different solvents. The absorbance of all solutions ranged between 0.1 – 0.15 at excitation wavelength. (Sharp signals observed in acetonitrile, dioxane and DMSO may be due to Raman scattering).

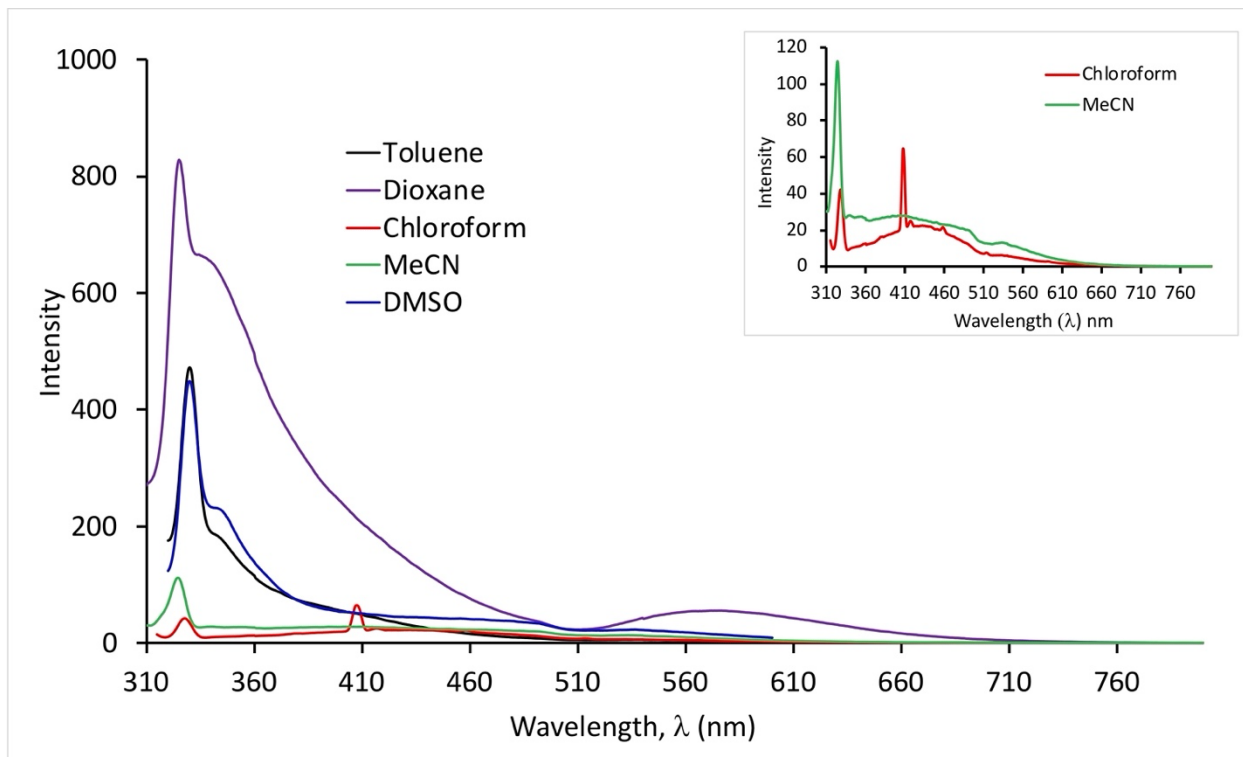


Figure S7. Emission spectra of **1b** in different solvents. The absorbance of all solutions ranged between 0.1 – 0.15 at excitation wavelength. (Sharp signals observed may be due to Raman scattering).

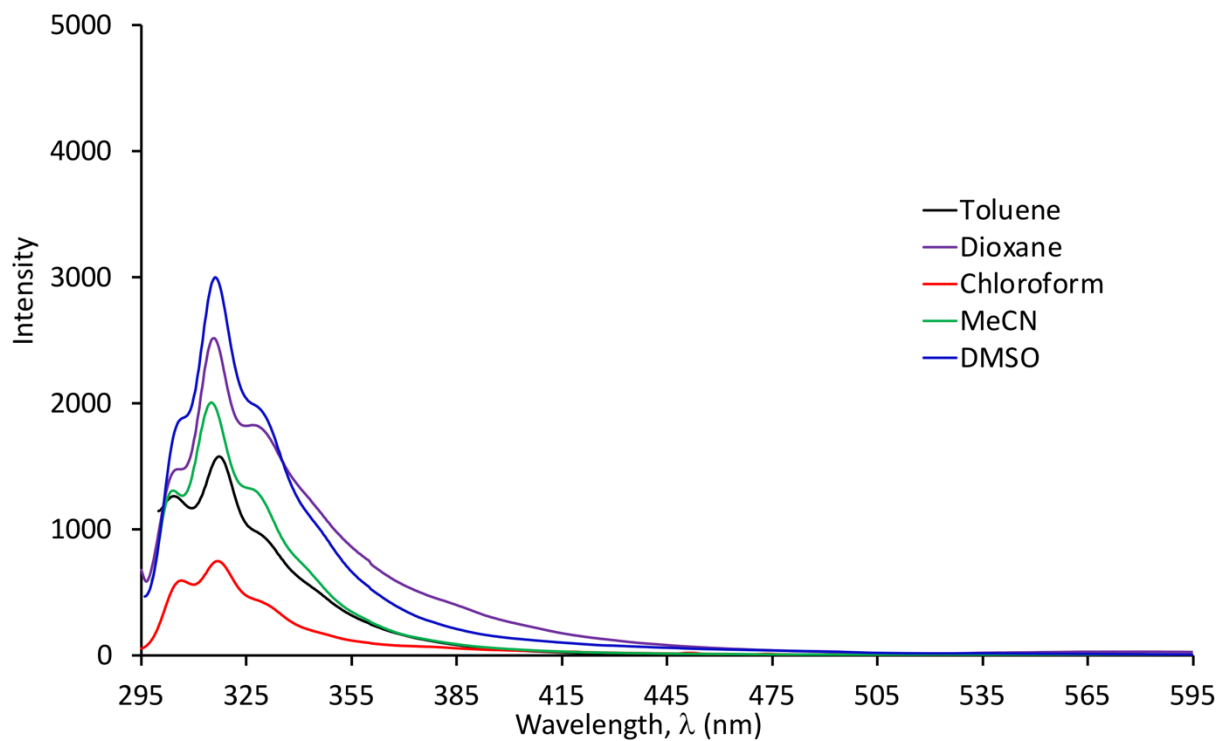


Figure S8. Emission spectra of **1c** in different solvents. The absorbance of all solutions ranged between 0.1 – 0.15 at excitation wavelength. The emission of **1c** was reproducible at different excitation wavelengths in all solvents.

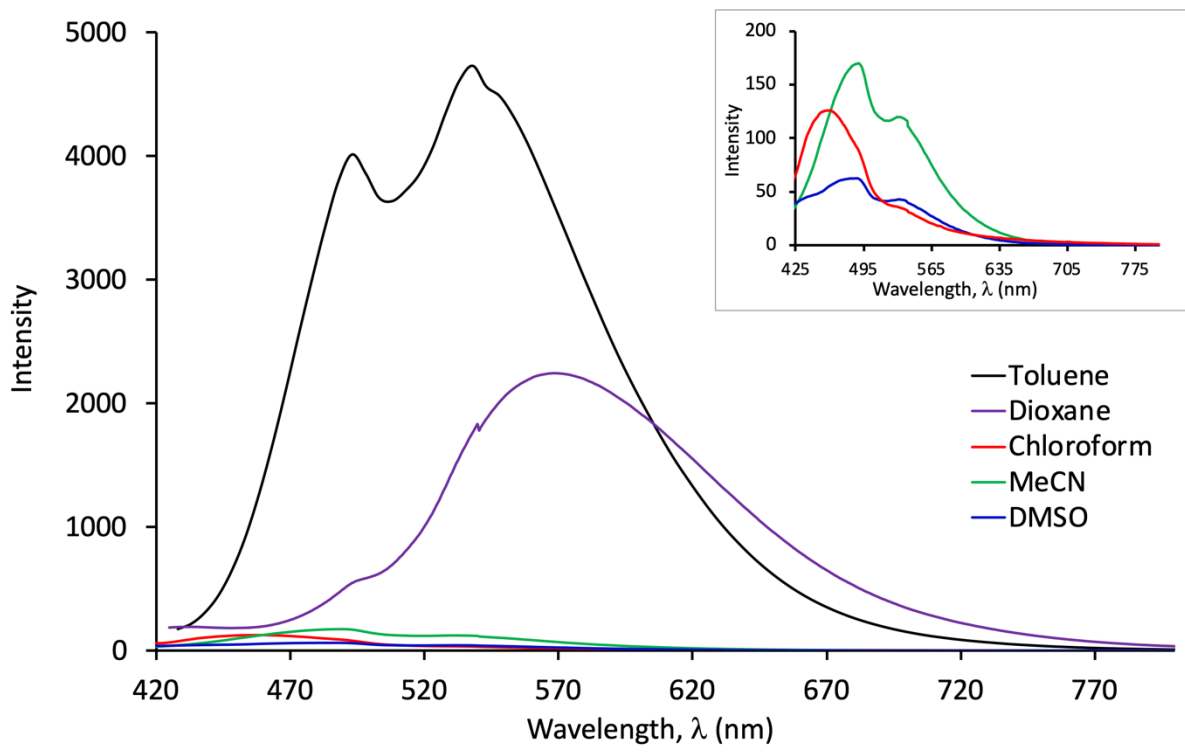


Figure S9. Emission spectra of **1d** in different solvents. The absorbance of all solutions ranged between 0.1 – 0.15 at excitation wavelength.

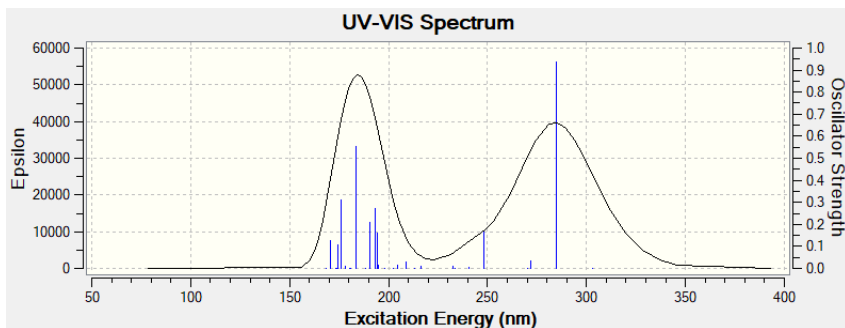


Figure S10. TDDFT (CAM-B3LYP/6-311++G**) simulated UV absorption spectrum of **1a** in acetonitrile.

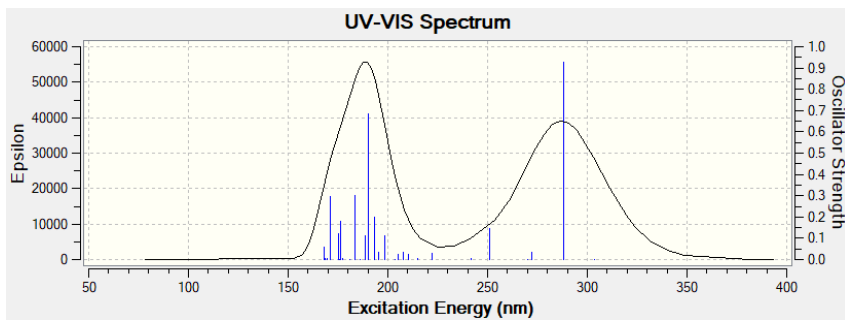


Figure S11. TDDFT (CAM-B3LYP/6-311++G**) simulated UV absorption spectrum of **1b** in acetonitrile.

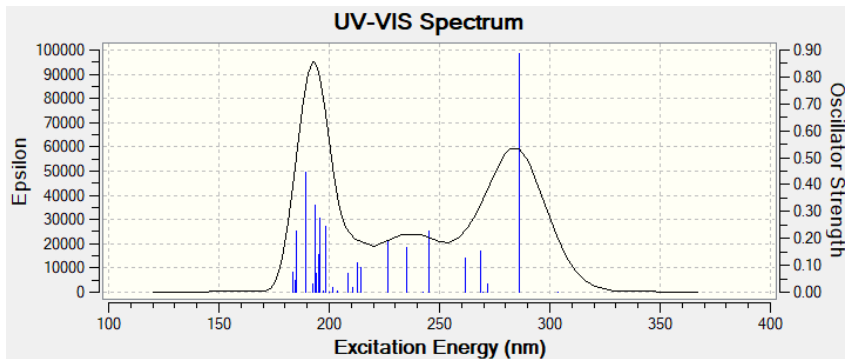


Figure S12. TDDFT (CAM-B3LYP/6-311++G**) simulated UV absorption spectrum of **1c** in acetonitrile.

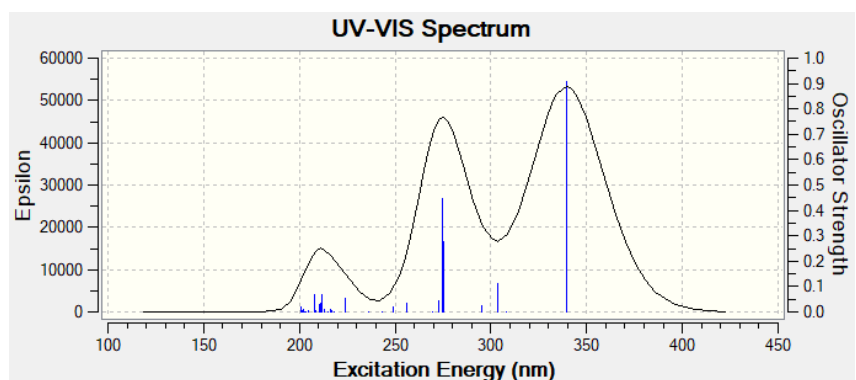


Figure S13. TDDFT (CAM-B3LYP/6-311++G**) simulated UV absorption spectrum of **1d** in acetonitrile.

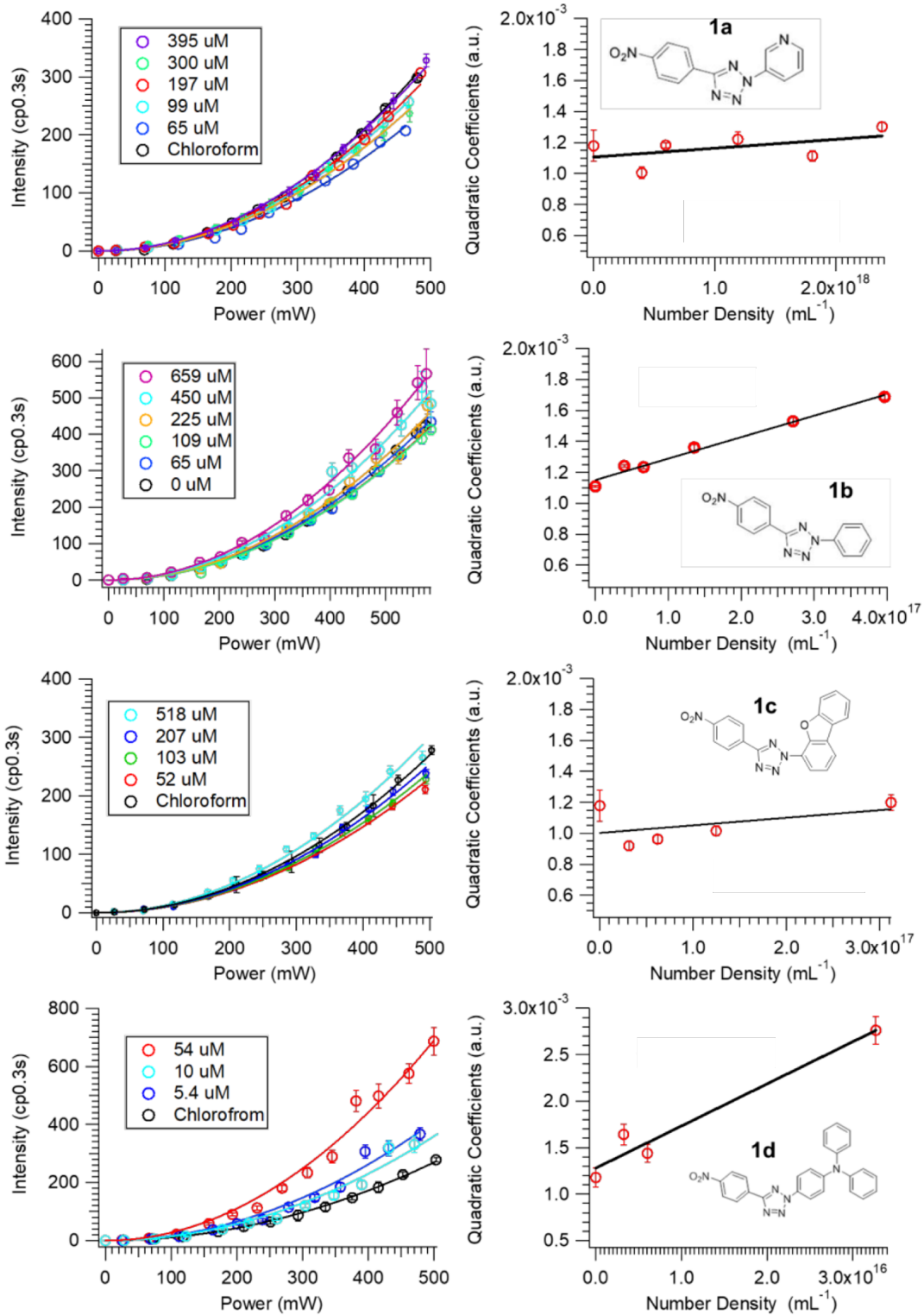
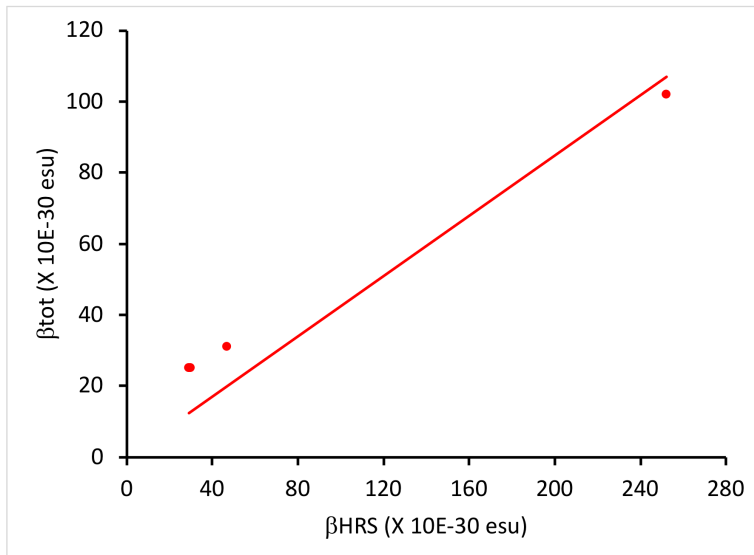


Figure S14. HRS data for compounds **1a – d**.



β_{tot}	25.4	31.3	25.2	101.6
β_{HRS}	30 ± 12	47 ± 2	30 ± 16	252 ± 16

Figure S15. Plot of β_{tot} Vs β_{HRS} showing a good correlation.

Table S1. UV absorption bands for **1a – d**, and the corresponding molar absorptivities.

		Toluene	Dioxane	CHCl ₃	MeCN	DMSO
1a	$\lambda_1^{\text{a}} (\varepsilon_1)^{\text{b}}$	Insoluble	296 (26719)	295 (24813)	293 (24593)	296 (19860)
	$\lambda_2^{\text{a}} (\varepsilon_2)^{\text{b}}$		-	-	195 (56904)	-
1b	$\lambda_1^{\text{a}} (\varepsilon_1)^{\text{b}}$	300 (21064)	295 (25138)	298 (23666)	295 (23216)	300 (21158)
	$\lambda_2^{\text{a}} (\varepsilon_2)^{\text{b}}$	-	-	-	195 (47751)	-
1c	$\lambda_1^{\text{a}} (\varepsilon_1)^{\text{b}}$	290 (28216)	288 (32865)	289 (26355)	287 (30363)	288 (28692)
	$\lambda_2^{\text{a}} (\varepsilon_2)^{\text{b}}$	-	253 (26635)	-	252 (25380)	-
	$\lambda_3^{\text{a}} (\varepsilon_3)^{\text{b}}$	-	-	-	199 (74787)	-
1d	$\lambda_1^{\text{a}} (\varepsilon_1)^{\text{b}}$	374 (19807)	368 (23217)	370 (18497)	360 (30186)	360 (18059)
	$\lambda_2^{\text{a}} (\varepsilon_2)^{\text{b}}$	293 (24966)	291 (29544)	294 (25308)	290 (36625)	293 (24877)
	$\lambda_3^{\text{a}} (\varepsilon_3)^{\text{b}}$				198 (153196)	

^a in nm; ^b M⁻¹ cm⁻¹

Table S2. TDDFT (CAM-B3LYP/6-311++G**) vertical excitation energies ($E(\lambda)$ / eV (nm)), oscillator strengths (f), MO character and transition type for **1a – d** as well as the transition dipole moment in acetonitrile.

		State	$E(\lambda)$	f	MO Character (%)	Type	μ_{eg}
Acetonitrile							
1a	λ_1	2	4.35 (285)	0.940	H→L (75%)	$\pi \rightarrow \pi^*/\text{CT}$	7.540
	λ_2	17	6.42 (193)	0.270	H-7→L (50%)	$\pi \rightarrow \pi^*/\text{CT}$	
		21	6.76 (183)	0.552	H-1→L+3 (44%)		
		25	7.03 (176)	0.312	H-1→L+4 (51%)		
1b	λ_1	2	4.30 (288)	0.929	H→L (67%)	$\pi \rightarrow \pi^*/\text{CT}$	7.542
	λ_2	17	6.51 (191)	0.682	H-3→L+1 (31%); H-2→L+1 (16%)	$\pi \rightarrow \pi^*/\text{CT}$	
		20	6.76 (183)	0.301	H-3→L+2 (39%)		
		27	7.24 (171)	0.294	H→L+10 (46%)		
1c	λ_1	2	4.33 (286)	0.887	H-2→L (45%); H-1→L (22%)	$\pi \rightarrow \pi^*/\text{CT}$	7.340
	λ_2	7	5.06 (245)	0.228	H→L (31%); H→L+2 (20%)	$\pi \rightarrow \pi^*/\text{CT}$	
		9	5.27 (235)	0.164	H-2→L+1 (17%); H-1→L (38%)		
		10	5.47 (227)	0.186	H→L+2 (31%)		
	λ_3	18	6.24 (198)	0.247	H-1→L+8 (24%)	$\pi \rightarrow \pi^*/\text{CT}$	
		20	6.34 (195)	0.277	H-1→L+8 (23%)		
		23	6.39 (194)	0.325	H-8→L (61%)		
		26	6.55 (189)	0.444	H-4→L+1 (26%)		
1d	λ_1	1	3.65 (340)	0.909	H→L (49%); H→L+1(37%)	$\pi \rightarrow \pi^*/\text{CT}$	8.098
	λ_2	5	4.50 (275)	0.275	H→L+5 (70%)	$\pi \rightarrow \pi^*/\text{CT}$	
		6	4.52 (274)	0.445	H-6→L (31%); H-1→L (27%)		
	λ_3	13	5.53 (224)	0.054	H-5→L+1 (22%)	$\pi \rightarrow \pi^*/\text{CT}$	
		20	5.85 (212)	0.066	H-1→L (33%)		
		24	5.97 (208)	0.066	H-3→L (29%)		

^a experimentally not observed.

Cartesian coordinates, total energies, and number of imaginary frequencies for 1a – d.

1a

Total Energy = -940.7143943 Hartrees

Number of Imaginary frequencies = 0

Cartesian coordinates of **1a** optimized at CAM-B3LYP/6-311++G**

0,1
C,-3.985422259,0.1982476799,0.0000741234
C,-3.5771654066,-1.1241143935,-0.0000420798
C,-3.0863961289,1.2513107802,0.0001287375
C,-2.2210621289,-1.3994527207,-0.0001024689
H,-4.3157456886,-1.9129373744,-0.0000829151
C,-1.7332161859,0.9661266026,0.0000664363
H,-3.4528018827,2.267894675,0.000219801
C,-1.2946671958,-0.3575911413,-0.000050844
H,-1.8699290146,-2.4227414383,-0.0001925053
H,-1.0088975261,1.7698096624,0.0001088122
N,2.1882444925,-0.507575108,-0.0000996932
N,1.1001826254,0.2428981434,0.0000234383
N,0.6409157302,-1.9206262308,-0.0002762768
C,0.1377512211,-0.6631608862,-0.0001189377
N,1.9287457823,-1.8039963776,-0.0003456951
C,3.508584469,0.0212438084,-0.000019743
C,4.6016366445,-0.8382574038,0.0005777798
C,3.7055445538,1.3917759075,-0.0005316162
H,4.4550765266,-1.9112976032,0.0010023975
H,2.8593608042,2.0648427231,-0.0009826645
C,6.0461868308,0.9264149286,0.0001483973
N,-5.4305107318,0.4975051464,0.000138912
O,-5.7628241263,1.6664378449,0.0002118445
O,-6.1998219195,-0.4427186256,-0.0000164974
H,7.0797639831,1.2558081006,0.0002186905
C,5.0109124369,1.8506912678,-0.0004343952
H,5.2236841265,2.9117301414,-0.00081723
N,5.8492789679,-0.3891531084,0.0006461918

1b

Total Energy = -924.6756471 Hartrees

Number of Imaginary frequencies = 0

Cartesian coordinates of **1b** optimized at CAM-B3LYP/6-311++G**

0,1
C,-3.9877874905,0.2026867934,-0.0000670121
C,-3.5835728436,-1.1212959905,0.0001162791
C,-3.0839056261,1.2519178505,-0.0002270216
C,-2.2286692266,-1.4016421007,0.0001385711
H,-4.3248219852,-1.9075869091,0.0002375635
C,-1.7318675985,0.9616035965,-0.0002030851
H,-3.4458868583,2.2700798594,-0.0003687642
C,-1.2978299089,-0.3636453936,-0.0000190534
H,-1.8812447872,-2.4262015352,0.000278448
H,-1.0042034577,1.7622543864,-0.0003265846
N,2.1848271455,-0.5197384768,0.0000570907
N,1.0978722278,0.2304472845,0.0000391575
N,0.6339036445,-1.9313578859,0.0000347162
C,0.1336232719,-0.6738783905,0.0000091074
N,1.9228538658,-1.8152351676,0.0000354039
C,3.5118353292,0.0062614483,0.0000848692
C,4.5885928705,-0.8695986004,0.0003866114
C,3.693076346,1.3810859708,-0.0001929036
H,4.4163149777,-1.9365834792,0.0006010162
H,2.8336862118,2.0363873538,-0.0004208169
C,6.0751454881,1.0265410028,0.0001261178
C,5.8722569386,-0.3473110561,0.0004014663
H,6.7190132556,-1.0222876341,0.0006351789
N,-5.430429226,0.5070217608,-0.0000898184
O,-5.7593319045,1.6773007162,-0.0002567672
O,-6.2041510469,-0.4301389484,0.0000237925
H,7.0814633952,1.4265228628,0.0001425077
C,4.9847869625,1.8853196544,-0.0001682213
H,5.1361390292,2.9575590274,-0.0003838488

1c

Total Energy = -1229.672058 Hartrees

Number of Imaginary frequencies = 0

Cartesian coordinates of **1c** optimized at CAM-B3LYP/6-311++G**

0,1
C,4.0317794076,2.7979681336,-0.7207747195
C,2.6633949172,2.8380738112,-0.462871325
C,1.9793451816,1.686327787,-0.1049261145
C,2.6917909209,0.5011202576,-0.0100484519
C,4.0638511131,0.4518695768,-0.2754464985
C,4.7418968545,1.610895595,-0.6344561931
H,4.5400920684,3.7123552522,-0.997822777
H,2.1145530152,3.7674597713,-0.5331163684
H,5.8051177601,1.589620969,-0.8388338323
C,3.2620182391,-1.5782518954,0.3266116891
C,3.1962533581,-2.9227665689,0.6334678556
C,4.3827007078,-3.6354489543,0.5459938852
C,5.5781550593,-3.0167951684,0.1663488558
C,5.6188044253,-1.6659551397,-0.1361669351
C,4.4381021249,-0.9329624044,-0.0545466761
H,2.2641594616,-3.3873798815,0.9260871551
H,4.3824152409,-4.693529477,0.7770039741
H,6.4848210894,-3.6059628943,0.1092750884
H,6.5485294099,-1.1935293607,-0.4288544435
O,2.1979980772,-0.7102414385,0.354724181
N,0.0314750461,2.7611733802,0.8100579663
N,-1.2349954543,2.5059400894,0.8658766095
N,0.5887205742,1.7408850026,0.1744904557
N,-0.2788109434,0.8148509272,-0.1929118431
C,-1.4186055088,1.3115548631,0.2545292664
C,-2.7209293376,0.6578696373,0.1057386389
C,-2.815861072,-0.5809521204,-0.5276736468
C,-3.8671949268,1.2778872842,0.6007699289
C,-4.0452937197,-1.1978741122,-0.6691174112
H,-1.9206391905,-1.0553701437,-0.9075622336
C,-5.1016880722,0.6679856981,0.4646750924
H,-3.781575909,2.2383776225,1.0912580376
C,-5.1688117422,-0.560982097,-0.1689372668
H,-4.1462281677,-2.1571141956,-1.156244687
H,-6.0051892484,1.1272520563,0.8393999125
N,-6.4816072092,-1.215165701,-0.3165173326
O,-7.4530647091,-0.6381614427,0.1314535167
O,-6.5144988417,-2.2932187191,-0.8775343531

1d

Total Energy = -1441.9602126 Hartrees

Number of Imaginary frequencies = 0

Cartesian coordinates of **1d** optimized at CAM-B3LYP/6-311++G**

0,1
C,3.9030424965,0.0801715566,-0.9362844563
C,3.5598466514,-1.2601243905,-0.8855334847
C,2.9768425118,1.0887466211,-0.729458382
C,2.2453336463,-1.5990508751,-0.6191192361
H,4.3163147655,-2.0133085203,-1.0533087647
C,1.6654295345,0.7397546437,-0.463448198
H,3.2905377625,2.1216345814,-0.7783266001
C,1.2929046642,-0.6029895134,-0.406902094
H,1.9456541703,-2.6375189203,-0.5725734039
H,0.9215853525,1.5075032109,-0.2966192403
N,-2.1082412361,-0.9089139967,0.2933740612
N,-1.0769718866,-0.1124500557,0.0808002671
N,-0.5299336675,-2.2516590531,-0.034232713
C,-0.094774573,-0.9758748847,-0.1236586654
N,-1.7988863347,-2.1911115371,0.2261169601
C,-3.4263346952,-0.4409801469,0.5675465966
C,-4.4102103602,-1.3415246401,0.9503026511
C,-3.7126163166,0.9103401062,0.449600286
H,-4.1720146958,-2.3914443593,1.0492606984
C,-4.9930334621,1.3618351356,0.7103593467
H,-2.9383308595,1.5993584759,0.1422741305
C,-6.001518527,0.4758718896,1.1020845004
H,-5.2166111587,2.414966819,0.6061426536
C,-5.6853500614,-0.8820548553,1.2188472429
H,-6.4477627707,-1.583753611,1.5289744639
N,5.3022825732,0.446777626,-1.2195316736
O,5.5788403638,1.6301097697,-1.2573336211
O,6.0966950321,-0.4555717356,-1.3985959564
N,-7.299358662,0.9373484676,1.3726618813
C,-7.5073210275,2.2300142082,1.9262972234
C,-8.4871705292,3.0676862395,1.3977057909
C,-6.7479342238,2.6680863257,3.0098182645
C,-8.7036470742,4.3220576883,1.9479216846
H,-9.0805343624,2.7284592756,0.5577326088
C,-6.95847803,3.9299131333,3.5444789685
H,-5.9922980125,2.0159386637,3.4301047672
C,-7.9384441753,4.7621728555,3.0195234522
H,-9.4694540231,4.9631011886,1.5277200947

H,-6.3610683657,4.2581309825,4.3867329463
H,-8.1055565356,5.7445139678,3.443631861
C,-8.4288018832,0.1160756246,1.1054278385
C,-8.5491499918,-0.5477324824,-0.1141259643
C,-9.4349956519,-0.0217082714,2.0591629141
C,-9.6532330469,-1.3475248068,-0.3666721448
H,-7.7734884665,-0.4353885684,-0.8615709651
C,-10.5446151811,-0.8099078554,1.793424786
H,-9.3446014805,0.4951505813,3.0064892688
C,-10.6576923985,-1.4804157433,0.5829897091
H,-9.7342699566,-1.8590992898,-1.3183593606
H,-11.3203714131,-0.9082333056,2.5434093115
H,-11.5223038181,-2.1002550295,0.3803227944

AW090319_CRUDE

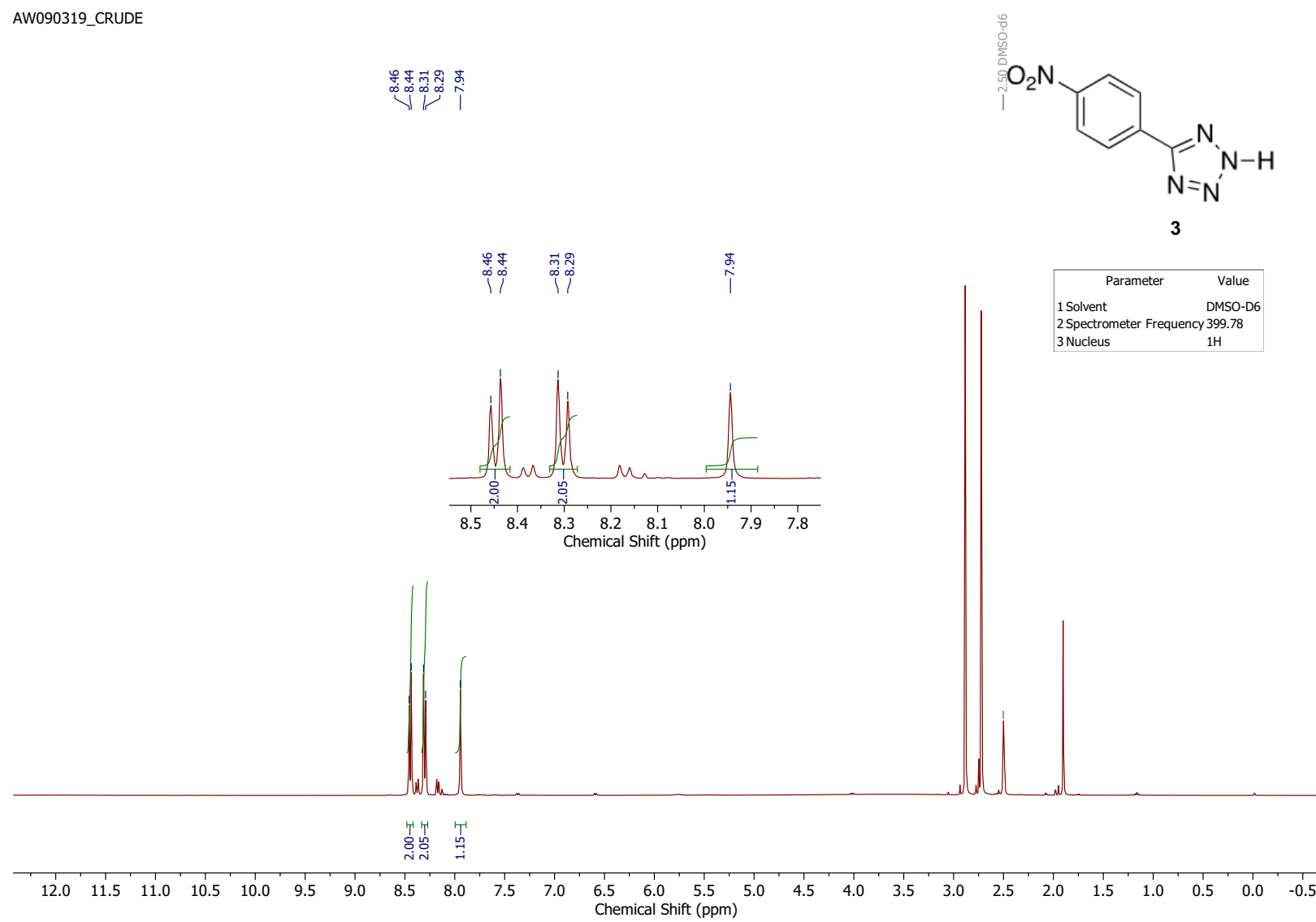


Figure S1. ^1H NMR spectra of **3** in $\text{DMSO}-d_6$

AW092519_PRODUCT

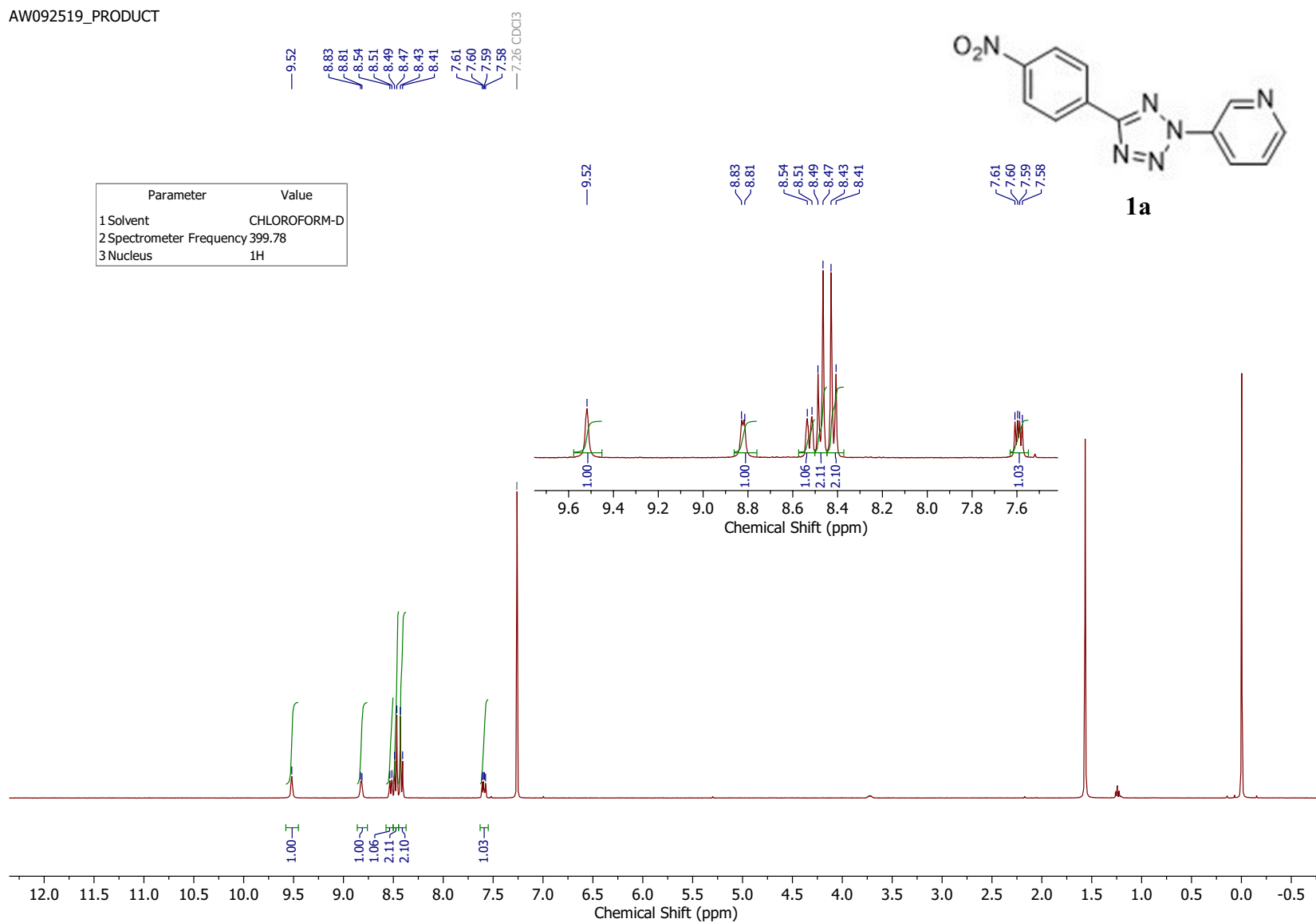


Figure S2. ¹H NMR spectra of **1a** in Chloroform-*d*

AW092519_PRODUCT

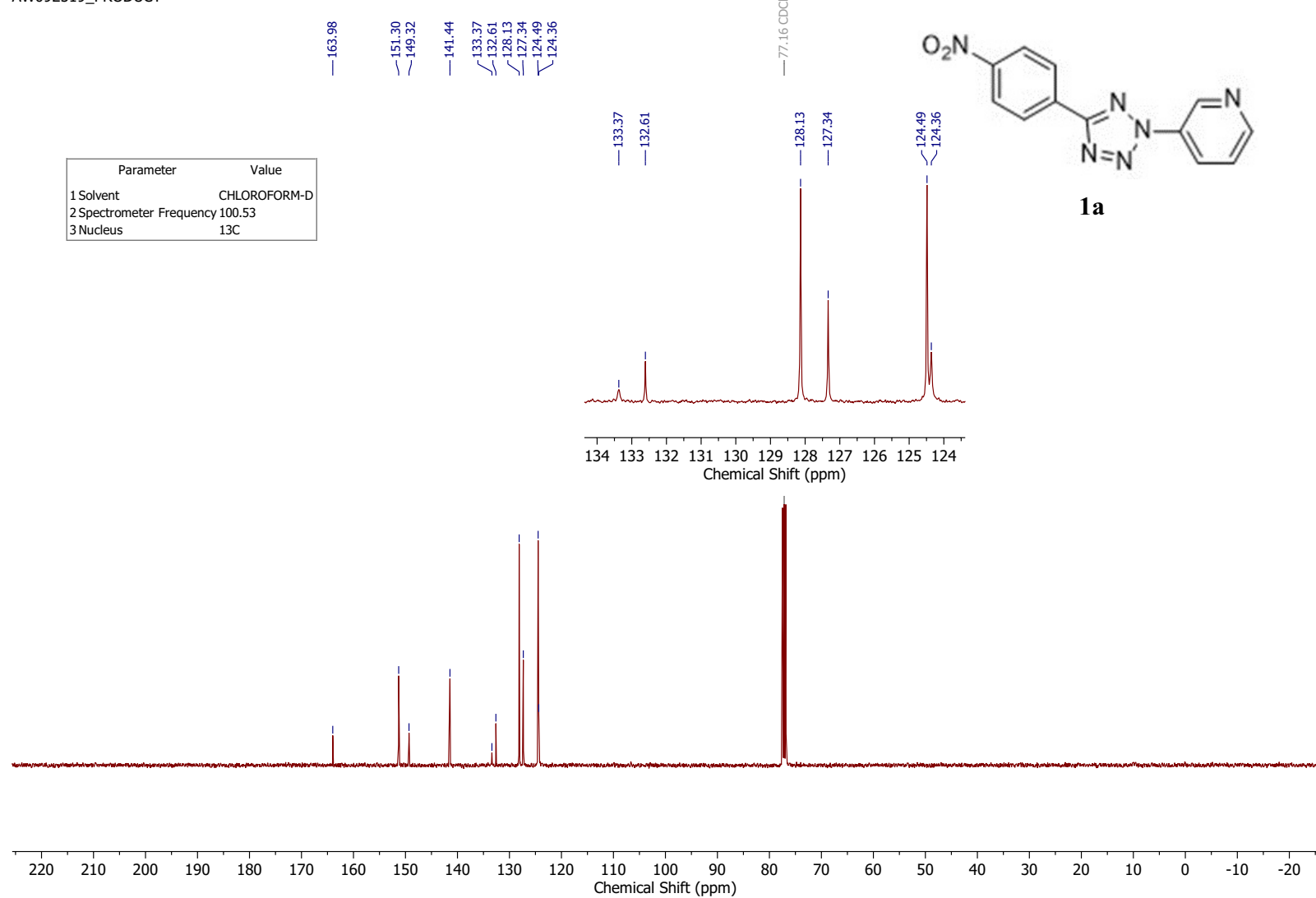


Figure S3. ¹³C NMR spectra of **1a** in Chloroform-*d*

AW062920_PROD_NO2_phenyl_recrys

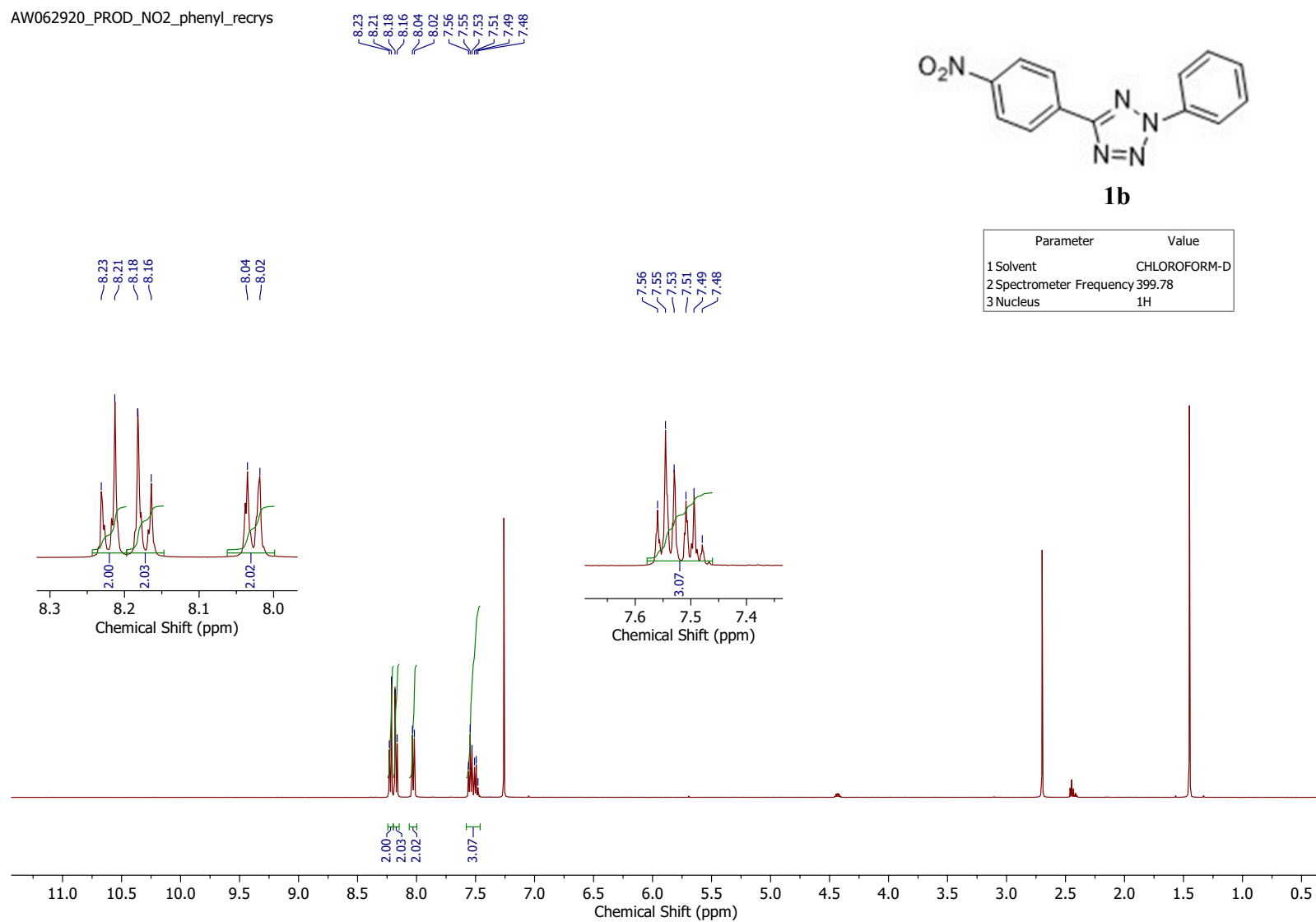


Figure S4. ¹H NMR spectra of **1b** in Chloroform-*d*

NO2_Phenyl_CDCL3

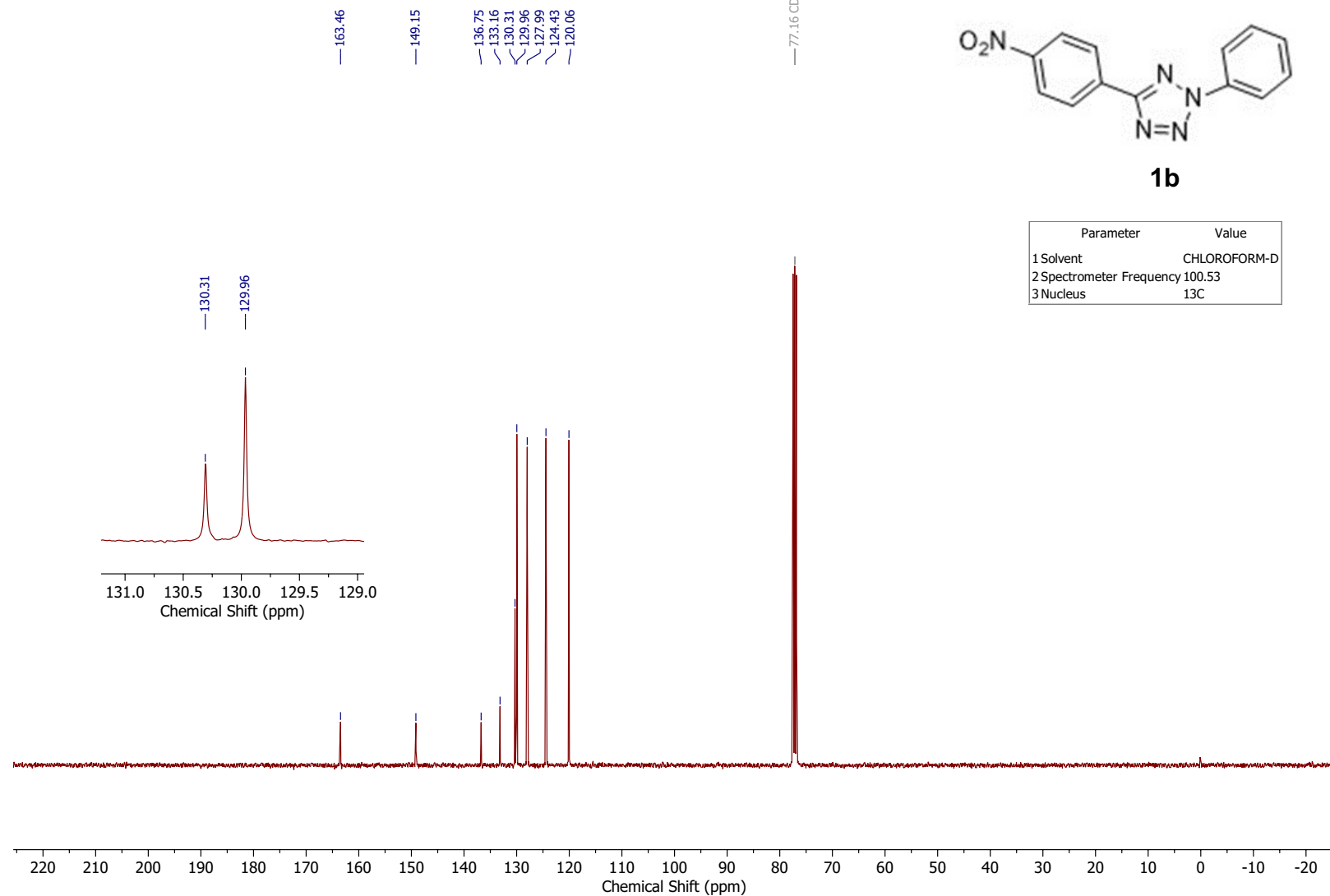


Figure S5. ^{13}C NMR spectra of **1b** in Chloroform-*d*

AW061120_PROD_NO2_Dibenzofuran_residue

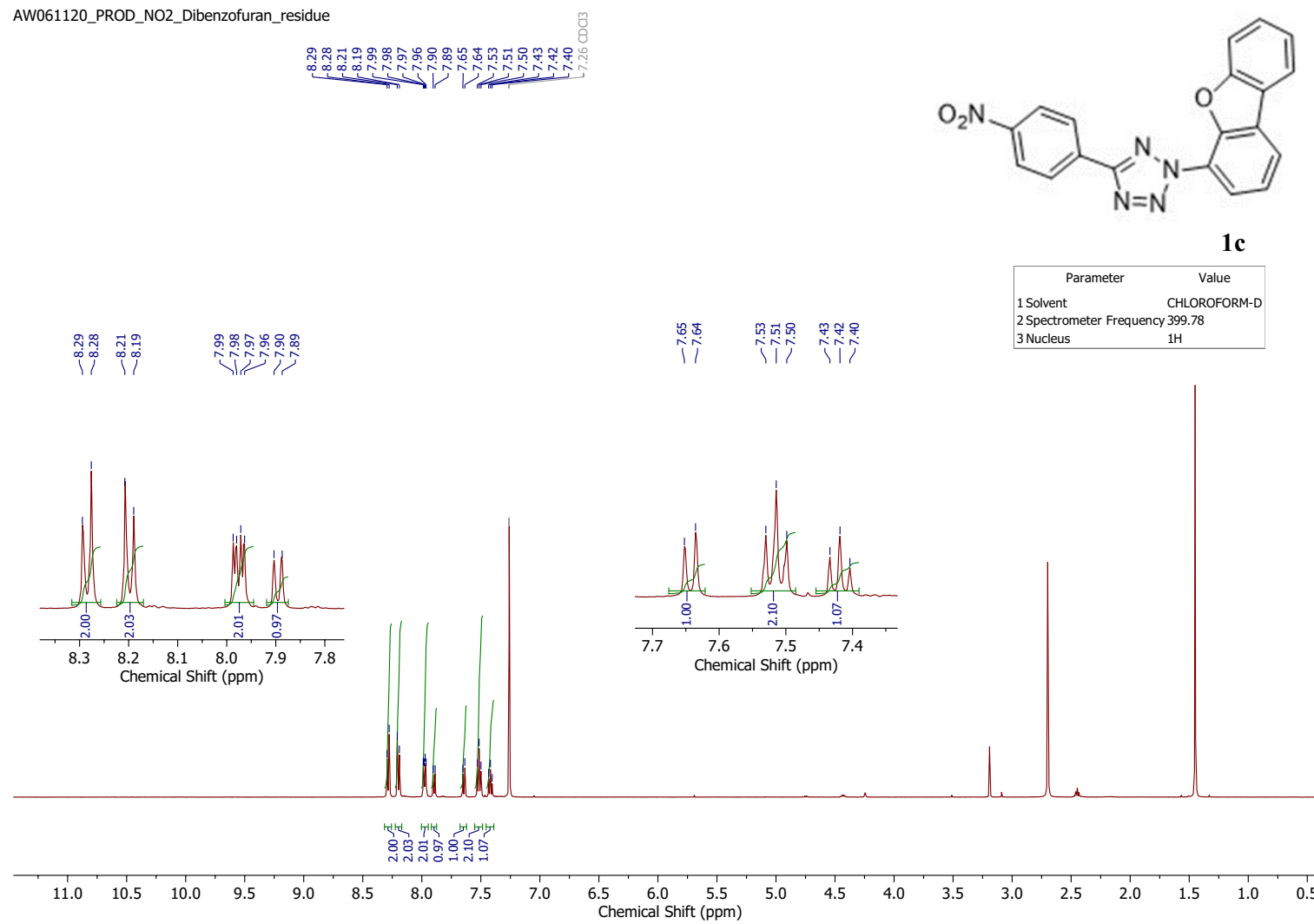


Figure S6. ¹H NMR spectra of **1c** in Chloroform-*d*

AW061120_PROD_NO2_dibenzofuran_residue

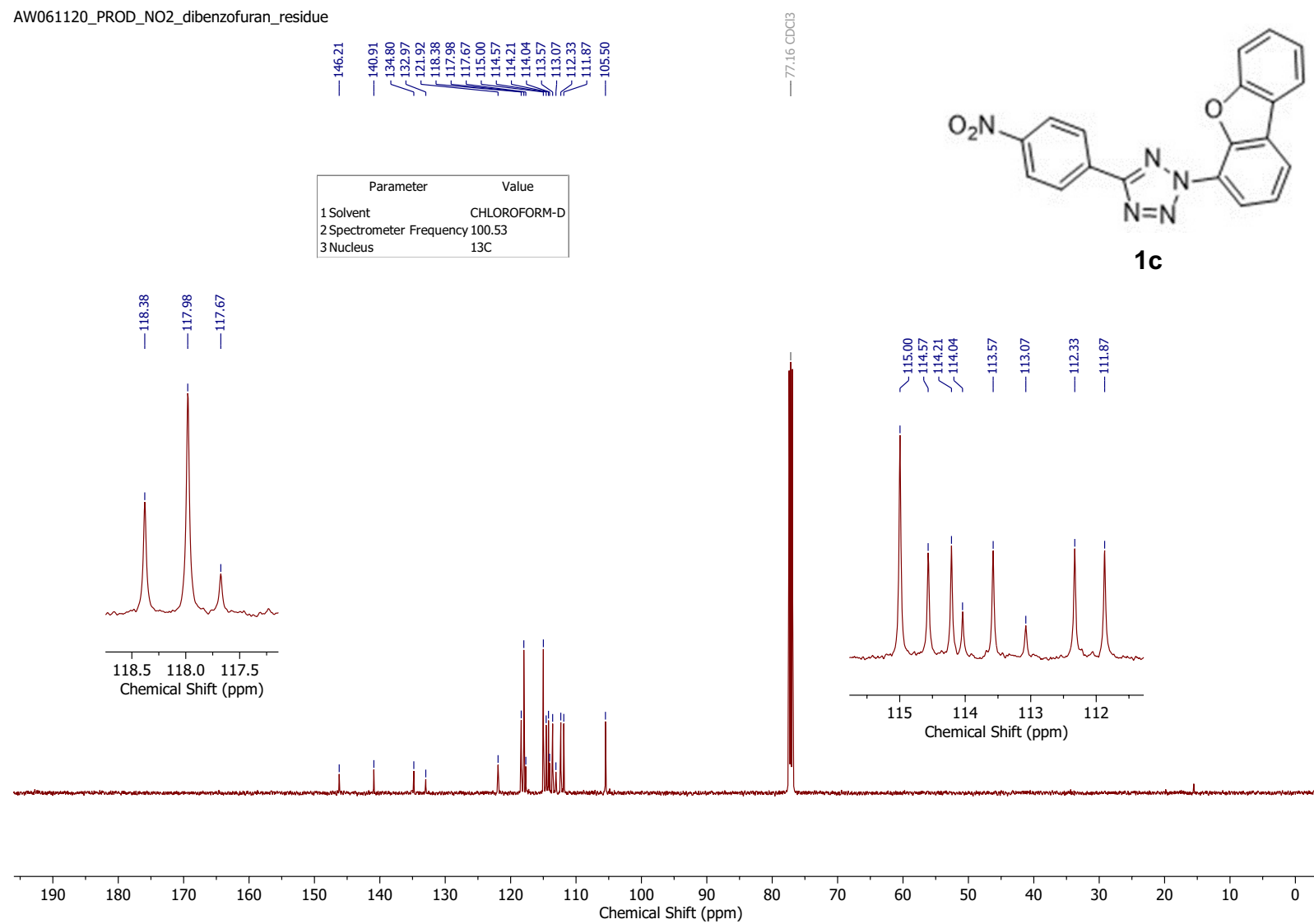


Figure S7. ^{13}C NMR spectra of **1c** in Chloroform-*d*

Residue_from_recrys

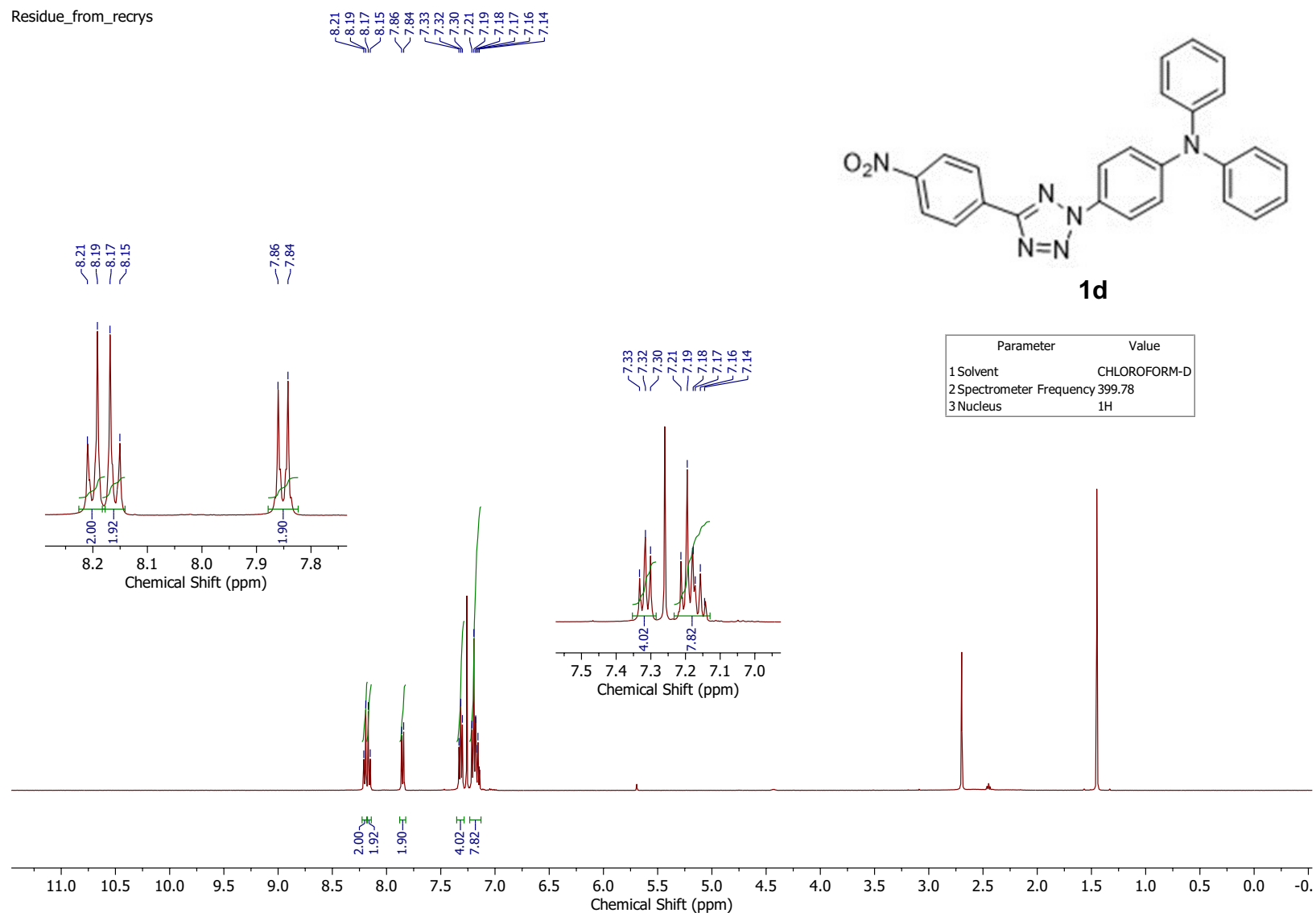


Figure S8. ¹H NMR spectra of **1d** in Chloroform-*d*

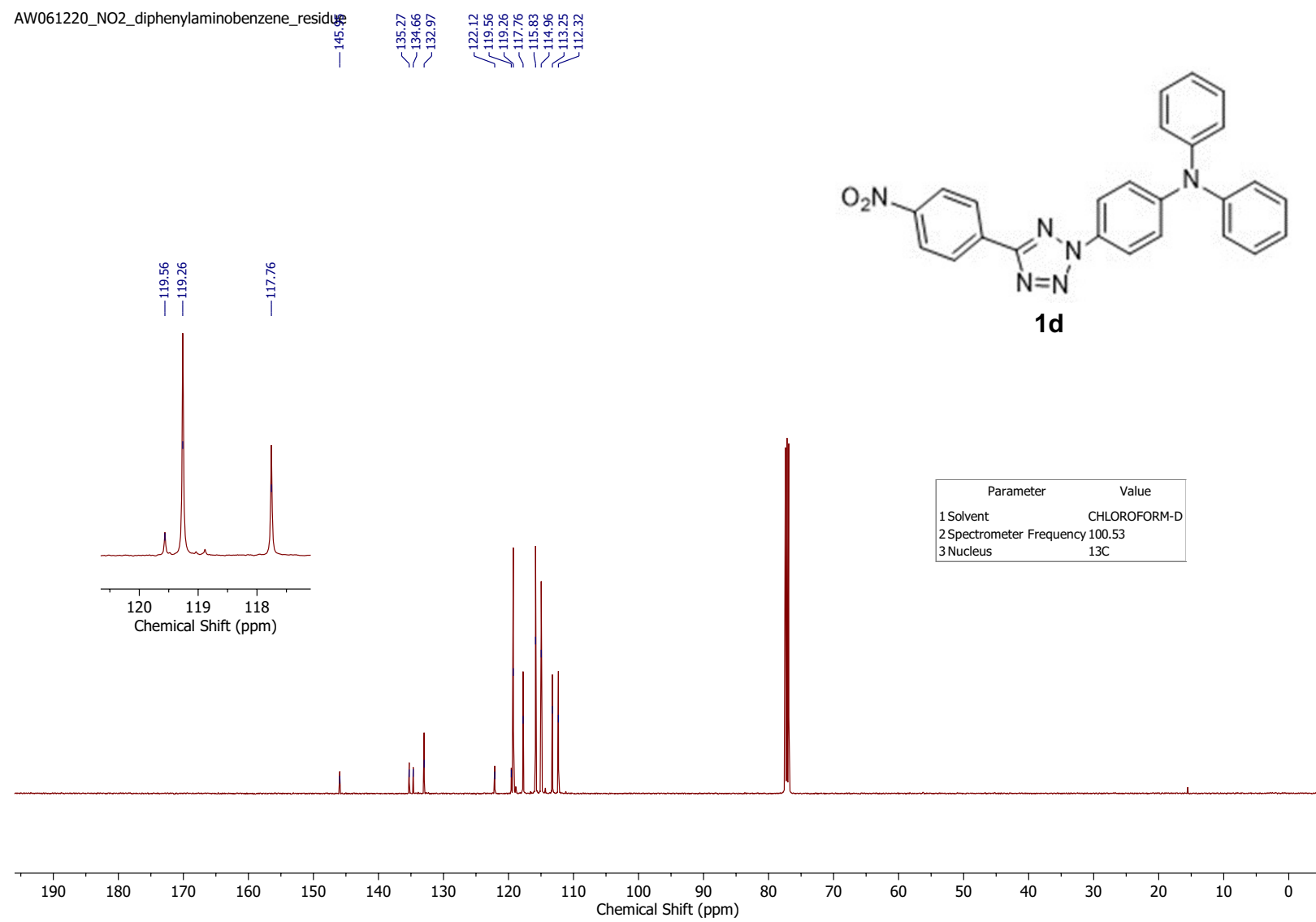


Figure S9. ^{13}C NMR spectra of **1d** in Chloroform-*d*